Migration of cobalt in nickel oxide/hydroxide active material of a nickel electrode in a Ni/H_2 cell

Hong S. Lim
Hughes Industrial Electronics Company, Building 231, MS 1921, 3100 Lomita Boulevard, Torrance, CA 90505 (USA)

Robert E. Doty
Hughes Research Laboratories, 3011 Malibu Canyon Road, Malibu, CA 90265 (USA)

(Received August 30, 1993; accepted in revised form November 15, 1993)

Abstract

We have studied cobalt distribution in nickel oxide/hydroxide active material in new nickel electrodes and those from Ni/H_2 cells which were subjected to long (229 to 565 days) storage tests. Three different energy dispersive X-ray analysis techniques, i.e., line scans, point-by-point analyses, and dot maps, combined with scanning electron microscopy clearly show that cobalt is redistributed in the microscopic region of the active material during the storage tests as reported earlier. Cobalt, which initially has a uniform distribution, becomes depleted near the interface between the active material and nickel metal particles of sintered plaque substrate and migrates into the bulk of active material. However, no correlation was found between the extent of the cobalt redistribution and the extent of capacity fading of the electrode during the storage tests, this in disagreement with earlier speculations. The present result enhances the possibility that a recovery method of the faded capacity can be developed.

Introduction

Capacity fading of Ni/H_2 cells on storage has been a problem for spacecraft applications. Some cells, after passing acceptance test, lose 20 to 40% of their capacity when stored for a period longer than two to three weeks [1]. Earlier studies indicated that the cause of capacity fading is closely related to changes in the distribution or oxidation state of the cobalt additive [1–3], since the cobalt additive has been known to improve the active material utilization of nickel electrodes [4, 5]. Migration of cobalt from the active material/nickel metal interface towards the bulk of the active material has also been observed in nickel electrodes which had suffered capacity fading [2, 3]. However, it has not been well established whether or not such cobalt migration is quantitatively related to the degree of capacity fading. The migration could conceivably occur during storage or cycling of Ni/H_2 cells without accompanying capacity fading. In this report, we characterize the cobalt migration under eleven different storage conditions for periods ranging from 229 to 565 days and compare the degree of capacity fading.

Experimental

The nickel electrodes used in this study are sintered types which are prepared by an electrochemical impregnation technique and are similar to those used in space Ni/H_2 cells [6]. The active material of nickel electrodes (designated as 'Co10') contained

Elsevier Sequoia
SSDI 0378-7753(94)01895-3

$11.7 \pm 0.5\%$ of cobalt additive (at.% of total nickel and cobalt) unless otherwise stated. Samples, Co7, BP3 and BP4 contained $9.3 \pm 0.8\%$ of cobalt and samples, Co4, BP5 and BP6 contained $6.7 \pm 0.8\%$ of cobalt. Both new electrodes and those tested in Ni/H_2 cells were studied for cobalt migration. The test history of electrodes investigated in this study is summarized in Table 1. Abbreviations in the Table are as follows: '26%' and '31%' denote the concentrations of KOH in the electrolyte for the Ni/H_2 cells in which the samples were tested. 'D/Al' and 'W/Al' represent the electrode types, i.e., 'D/Al' for those made of a dry-powder sintered plaque substrate and made by an alcoholic bath process [6] and 'W/Al' similar electrode but made of a wet-slurry sintered plaque. Further details of the history of the electrodes were described in refs. 2 and 7.

Metallographic specimens of nickel electrode samples were prepared by using an epoxy potting technique to study cross-sectional areas of the electrode. Techniques used to analyze the cobalt distribution were scanning electron microscopy (SEM) and energy dispersive X-ray (EDX) analysis. After coating specimens with carbon to prevent charging, the samples were examined in a Hitachi S-800 SEM which is fitted with a KEVEX Delta IV EDX analyzer. Analysis was carried out using a 20 keV electron beam with a sample working distance of 25 mm. The ultra-thin window of the EDX detector makes it possible to detect light elements down to boron, and a fast X-ray mapping module allows simultaneous mapping of several elements into individual image arrays of 256×128 pixels. Semi-quantitative elemental composition was determined without use of standards by ZAF correction computer program. The cobalt concentrations and distributions in microscopic areas were characterized by EDX line scans, point-by-point analyses, and Ni, Co and O dot mapping.

TABLE 1

Summary of storage test history of nickel electrodes in Ni/H_2 cell

Electrode identification	Storage test history[a]	Initial capacity[b] (Ah)	Final capacity[b] (% of initial value)
Co10 (new)			
Co7 (new)			
Co4 (new)			
W/Al (new)			
BP1 (Co10, 26%)	565 days H_2	5.08	94.1
BP3 (Co7, 26%)	565 days H_2	5.47	89.8
BP5 (Co4, 26%)	565 days H_2	5.80	91.2
BP2 (Co10, 26%)	146 days Ni/142 days O/277 days H_2	4.95	116.0
BP4 (Co7, 26%)	146 days Ni/142 days O/277 days H_2	5.48	102.0
BP6 (Co4, 26%)	146 days Ni/142 days O/277 days H_2	5.89	90.8
BP8 (D/Al, 31%)	229 days H_2	4.85	54.4
BP9 (D/Al, 31%)	229 days TC/134 days O	4.93	77.5
BP3b (W/Al, 26%)	268 days H_2	3.41	51.6
BP4b (D/Al, 26%)	268 days O	4.96	76.0
BP4c (D/Al, 26%)	268 days H_2	4.90	40.4

[a]H_2: under H_2 precharge; Ni: under nickel precharge; O: under no precharge (vacuum); and TC: trickle charging.

[b]Capacity measurement by $C/10$ rate charge for 18 h followed by discharge at $C/2$ rate to 1.0 V.

Results and discussion

A typical cross-section view of a nickel electrode at ×500 is shown in Fig. 1. Bright areas represent nickel sinter particles and grey areas represent nickel oxide/hydroxide active material which contained cobalt oxide additive. We have studied cobalt distributions in the active material between two nickel particles which are approximately 10 μm apart in nickel electrode samples which were subjected to storage tests in a Ni/H_2 cell as described in Table 1.

EDX line scan

EDX line scan results for new electrodes are shown in Fig. 2. In these new electrodes, cobalt concentration was evenly distributed across an approximately 10 μm region of the active material between nickel metal particles. Results for the electrodes tested in Ni/H_2 cells (BP8 and BP2) are shown in Fig. 3. The cobalt distributions in these electrodes are not uniform across the region. Cobalt concentration is high in the bulk of the active material and low near nickel metal particles. These results indicate that cobalt migrates in the active material from interfacial areas of the nickel metal particles of the substrate towards the bulk during storage of Ni/H_2 cells.

Point-by-point EDX analysis

Results of point-by-point analysis results of cobalt distribution for those electrodes used for Figs. 2 and 3 are shown in Figs. 4 and 5. Overall results are identical to those of the line scan. Cobalt concentration is high in the bulk of the active material and low near nickel metal particles in the BP8 and BP2 electrodes while it is evenly distributed in the new electrodes. Cobalt concentrations shown in Fig. 4 are in good agreement with results of our chemical analysis, i.e., 11.8, 9.9 and 6.8% for Co10, Co7 and Co4 electrodes, respectively. The concentrations in the storage tested samples (which are otherwise similar to Co10) in the middle region were as high as 22 to 26% while these values near the interface were below the average value of 12%

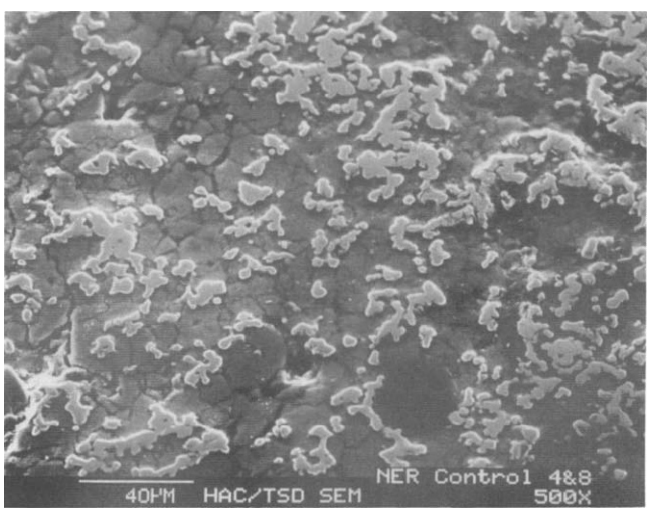

Fig. 1. SEM picture of a typical cross-sectional area of a sintered type nickel electrode; magnification ×500.

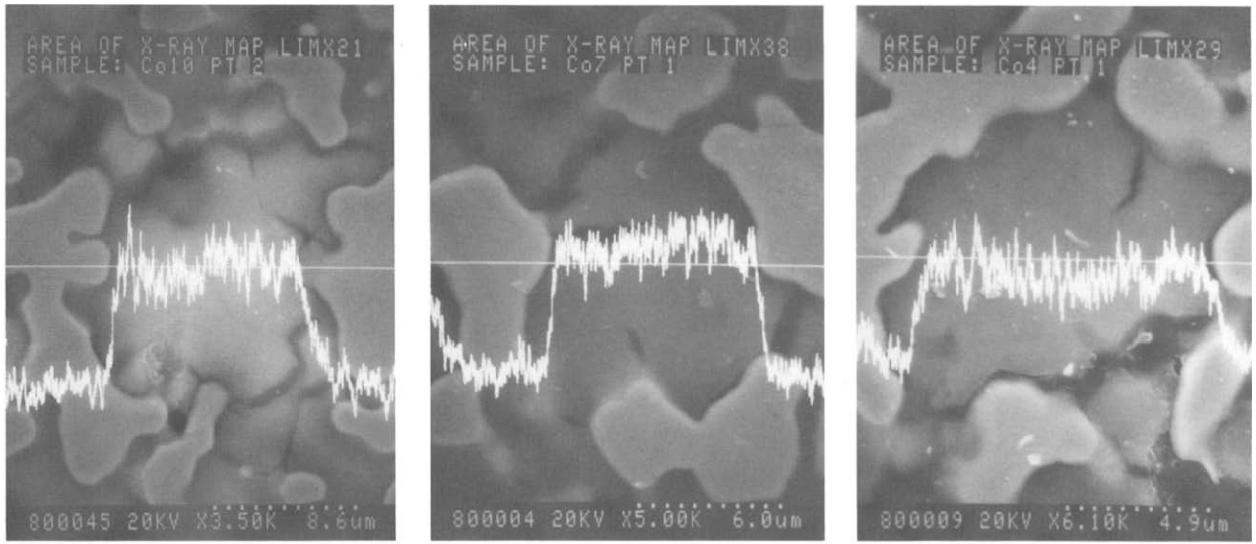

(a) (b) (c)

Fig. 2. SEM pictures and EDX cobalt line scan results of metallographic samples of new nickel electrodes: (a) Co10; (b) Co7, and (c) Co4. Light colored islands in the picture are nickel metal particles and remaining grey areas represent active material.

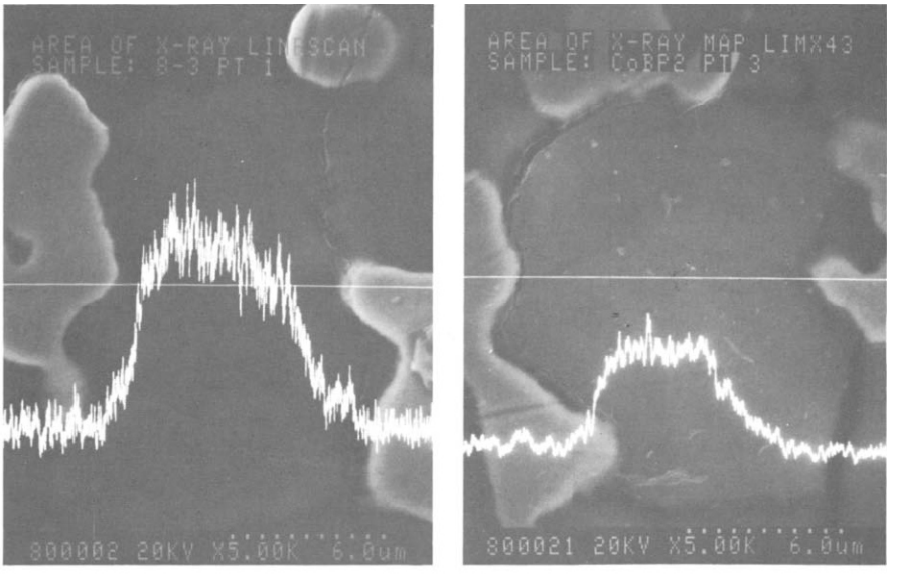

(a) (b)

Fig. 3. SEM pictures and EDX cobalt line scan results of metallographic samples of nickel electrodes from (a) BP8 and (b) BP2. Light colored islands in the picture are nickel metal particles and remaining grey areas represent active material.

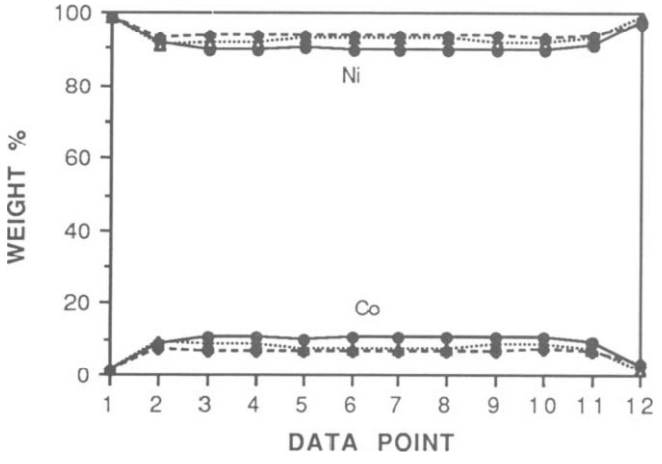

Fig. 4. Point-by-point analysis results of cobalt and nickel for (●) Co10, (△) Co7, and (◆) Co4 in the similar region as the EDX line scan.

(Fig. 5). These results also indicate that cobalt has migrated from the interface between the active material and nickel metal particles of sintered plaque into the bulk of the active material during storage test periods.

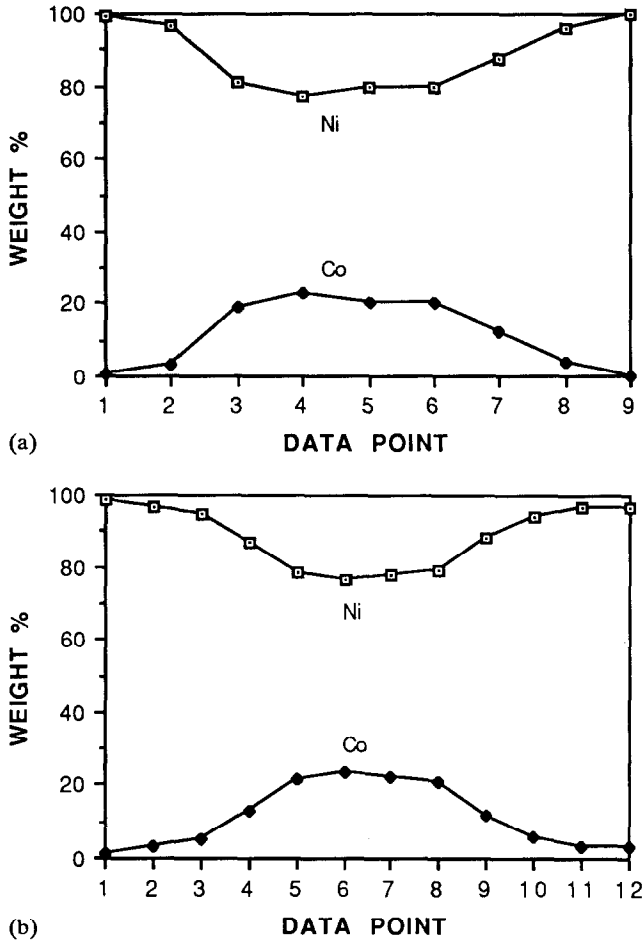

Fig. 5. Point-by-point analysis results of cobalt and nickel (a) BP8 and (b) BP2 in the similar region as the EDX line scan.

Ni, Co and O dot maps

Scanning electron microscopy images of the electrode cross section (magnified approximately ×3000) and dot maps of Ni, Co and O for a new Co10 electrode are shown in Fig. 6. The bright areas in these elemental maps represent a high concentration of the corresponding elements. All dot maps match well with the SEM images of the corresponding samples for new electrodes: the Ni maps show high concentrations of Ni in the area where Ni metal particles are while low concentrations are shown where the active material is shown by the SEM image. The Co maps show low concentrations in the area where Ni metal particles are while high concentrations are shown where the active material is shown by the SEM image. Similarly the O maps show low concentrations in the area where Ni metal particles are while high concentrations are shown where the active material is shown by the SEM image. These observations show that cobalt is distributed evenly in the active material of the new electrodes.

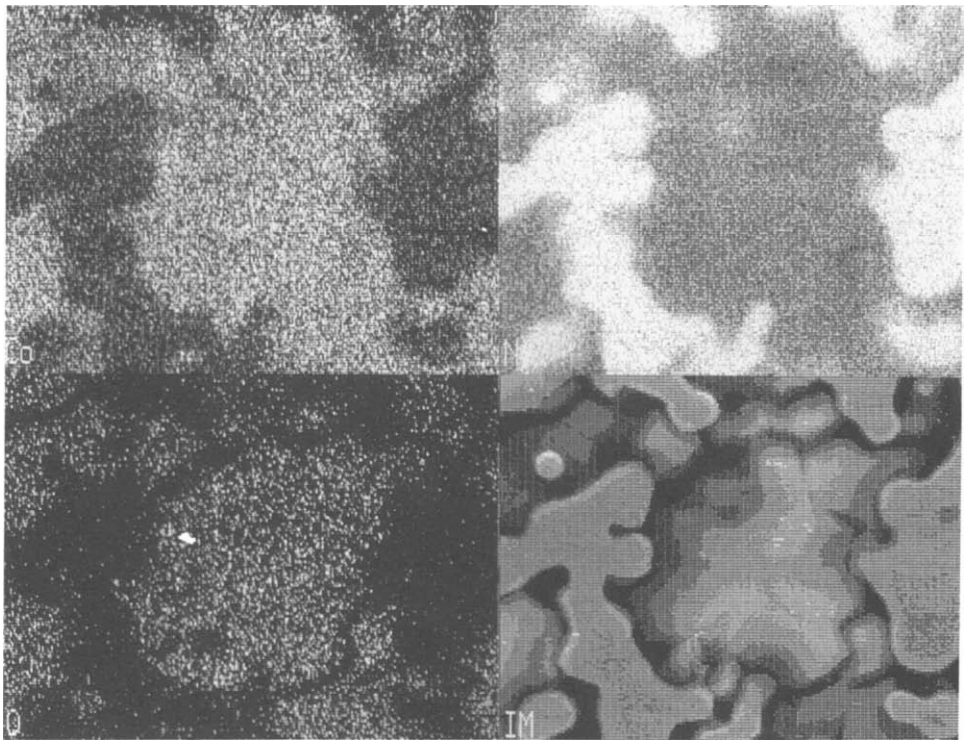

Fig. 6. SEM images (lower right), EDX maps of Ni (upper right), Co (upper left) and O (lower left) for Co10. Brightness of areas represents the concentration of the corresponding elements.

The SEM images of the electrode cross section and dot maps for a new Co7 and Co4 electrodes (not shown) were similar to those of the Co10 electrode.

Similar SEM images of the electrode cross section and dot maps of Ni, Co, and O for the BP8 and BP2 electrodes are shown in Figs. 7 and 8. Nickel and O maps also match well with the SEM images for these electrodes, but Co maps do not match with the SEM image. The area of the high Co region is noticeably smaller than that of the active material in the SEM image indicating the cobalt has redistributed in a manner similar to that indicated by the line scan and point-by-point analysis results.

All these results clearly show that cobalt has migrated from the interface between the active material and nickel metal particles of sintered plaque towards the bulk of active material in the BP8 and BP2 electrodes which were subjected to a storage test for over 200 days in a Ni/H_2 cell. Observations on other electrodes are summarized in Table 2. Other storage-tested electrodes also showed Co migration even though the extent of migration varied with the sample test history. Two different possible mechanisms have been suggested earlier: Zimmerman [3] proposed that the cobalt segregation occurs through a slow electrochemical reduction of cobalt hydroxide to cobalt metal at the nickel metal (current collector) surface in the presence of excess hydrogen while the cobalt metal can be re-oxidized to cobalt hydroxide without detailed explanation of a physical segregation mechanism. Lim [2] suggested an alternate mechanism as follows: cobalt stays in oxidation(III) state as long as there is some nickel(III) around the cobalt as is the case in usual charged and discharged state.

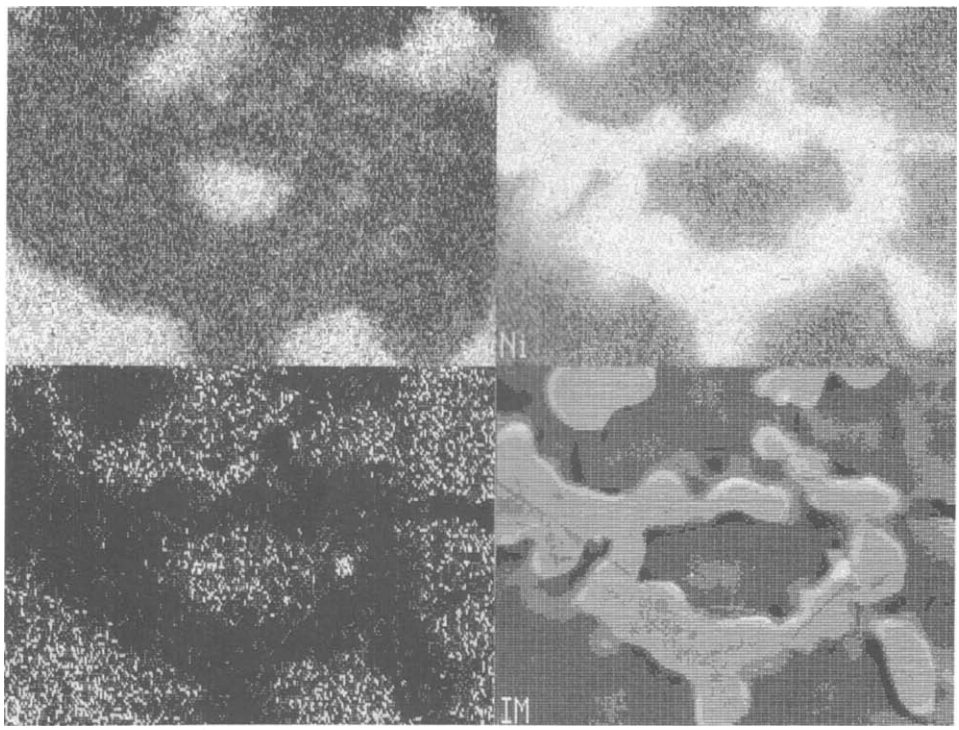

Fig. 7. SEM images and EDX maps of Ni, Co and O for BP8.

However, on a prolonged storage of a discharged Ni/H_2 cell, cobalt(III) in the active material near the nickel metal surface will be reduced to cobalt(II) which is slightly soluble by the formation of an anion ($HCoO_2^-$). These ions will migrate away from the surface towards the bulk of the active material either by migration or by diffusion process.

In Table 3, semi-quantitative results of the cobalt redistribution for all the storage-tested electrodes are summarized and compared with the extent of the capacity fading in the Ni/H_2 cell during the storage test. Earlier, there were attempts to correlate capacity fading with the cobalt migration [2, 3]. However, such correlation was not confirmed by the present result. BP2 and BP4 did not suffer capacity fading at all but showed the most severe cobalt redistribution, while BP3b, BP4b, and BP4c suffered severe capacity fading but showed only mild cobalt redistribution.

Summary

It is confirmed that the migration of cobalt into the active material of nickel electrodes occurs during storage of Ni/H_2 cells as reported earlier [2, 3]. The direction of migration is from the interface between the active material and nickel metal particles of sintered plaque into the bulk of active material. However, there was no direct correlation between capacity fading and redistribution of cobalt. Although the mechanism of capacity fading is not well understood, the present result has an important practical implication. If capacity fading was due solely to the redistribution of cobalt as speculated

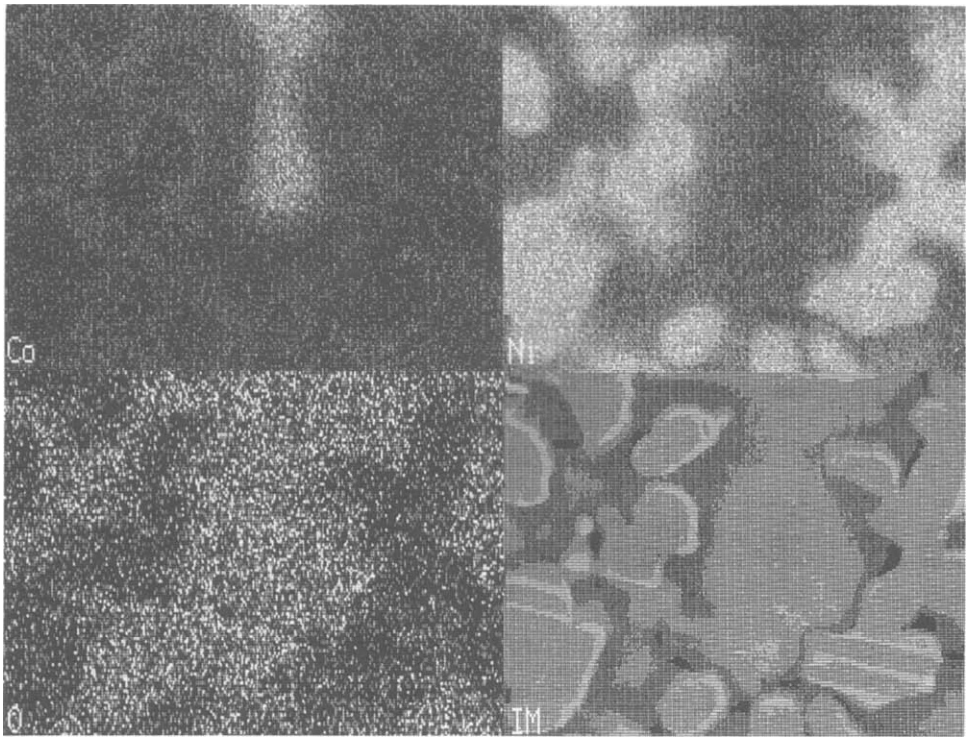

Fig. 8. SEM images and EDX maps of Ni, Co and O for BP2.

TABLE 2

Summary of scanning electron microscopy and energy dispersive X-ray observations on nickel electrodes of various tests histories

Electrode identification	Dot-by-dot results		Line scan results	Dot mapping results
	Peak % Co	Distribution		
Co10	11–14	Flat	Flat	Match SEM
Co7	7–11	Flat	Flat	Match SEM
Co4	5–8	Flat	Flat	Match SEM
W/Al	10–14	Flat	Flat	Match SEM
BP1 (Co10, 26%, H_2)	14–16	Flat	Flat	Co $\leqslant$ Ni–O
BP3 (Co7, 26%, H_2)	14–17	Slightly parabolic	Flat	Co $\leqslant$ Ni–O
BP5 (Co4, 26%, H_2)	8–14	Flat	Flat	Co $\leqslant$ Ni–O
BP2 (Co10, 26%, Ni)	23–26	Parabolic	Parabolic	Co < Ni–O
BP4 (Co7, 26%, Ni)	14–20	Slightly parabolic	Slightly parabolic	Co < Ni–O
BP6 (Co4, 26%, Ni)	6–13	Slightly parabolic	Slightly parabolic	Co < Ni–O

(*continued*)

TABLE 2 (*continued*)

Electrode identification	Dot-by-dot results		Line scan results	Dot mapping results
	Peak % Co	Distribution		
BP8 (D/Al, 31%, H_2)	22–24	Parabolic	Parabolic	Co<Ni–O
BP9 (D/Al, 31%, O)	14–19	Flat	Flat	Co<Ni–O
BP3b (W/Al, 26%, H_2)	22–26	Slightly parabolic	Slightly parabolic	Co<Ni–O
BP4b (D/Al, 26%, O)	14–15	Flat	Flat	Co≤Ni–O
BP4c (D/Al, 26%, H_2)	20–21	Parabolic	Parabolic	Co<Ni–O

TABLE 3

Comparison of cobalt redistributions and cell storage history

Electrode identification	Capacity fade (% of initial volume)	Peak % Co	Severity of Co redistribution (0–10)[a]
BP1 (Co10, 26%, H_2	94.1	14–16	2
BP3 (Co7, 26%, H_2)	89.8	14–17	2
BP5 (Co4, 26%, H_2)	91.2	8–14	2
BP2 (Co10, 26%, Ni)	116.0	23–26	10
BP4 (Co7, 26%, Ni)	102.0	14–20	9
BP6 (Co4, 26%, Ni)	90.8	6–13	8
BP8 (D/Al, 31%, H_2)	54.4	22–24	6
BP9 (D/Al, 31%, O)	77.5	14–19	4
BP3b (W/Al, 26%, H_2)	51.6	22–26	4
BP4b (D/Al, 26%, O)	76.0	14–15	2
BP4c (D/Al, 26%, H_2)	40.4	20–21	4

[a]Visual determination by the shrinkage of Co area from the dot maps.

earlier [2, 3], it might be extremely difficult to develop a method for capacity recovery because even a conceptual method is not available for restoring the original uniform distribution of cobalt. The present results appear to show a possibility for development of a capacity recovery technique of a capacity faded cell, for example, as indicated by a partial recovery of the faded capacity by low temperature (0 °C) cycling [7].

References

1 H.S. Lim and S.J. Stadnick, *J. Power Sources, 27* (1989) 69.
2 H.S. Lim and S.A. Verzwyvelt, *Proc. 25th Intersociety Energy Conversion Engineering Conf., Reno, NV, USA, Aug. 12–17, 1990,* Vol. 3, p. 7.
3 A.H. Zimmerman and R. Seaver, *J. Electrochem. Soc., 137* (1990) 2662.
4 S. Januszkiewicz, *Proc. 13th Annual Power Sources Conf., Atlantic City, NJ, USA, Apr. 28–30, 1959,* p. 75.
5 H. Yasuda, K. Iwai and J. Takeshima, *Denshi Toronkai, 18* (1979) 89.
6 D.F. Pickett, H.H. Rogers, L.A. Tinker, C.A. Bleser, M. Hill and J. S. Meador, *Proc. 15th Intersociety Energy Conversion Engineering Conf., 1980,* p. 1918.
7 H.S. Lim, *Proc. 27th Intersociety Energy Conversion Engineering Conf., Aug. 1992,* Vol. 1, p. 239.